

Binding Modes of Thioflavin T Molecules to Prion Peptide Assemblies Identified by Using Scanning Tunneling Microscopy

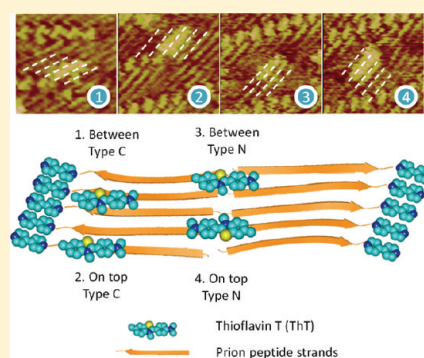
Xiaobo Mao, Yuanyuan Guo, Chenxuan Wang, Min Zhang, Xiaojing Ma, Lei Liu, Lin Niu, Qingdao Zeng, Yanlian Yang,* and Chen Wang*

Key Laboratory for Biological Effects of Nanomaterials & Nanosafety and Key Laboratory of Standardization and Measurement for Nanotechnology (Chinese Academy of Sciences) National Center for Nanoscience and Technology, 11 Beiyitiao, Zhongguancun, Beijing 100190, P. R. China

Supporting Information

ABSTRACT: The widely used method to monitor the aggregation process of amyloid peptide is thioflavin T (ThT) assay, while the detailed molecular mechanism is still not clear. In this work, we report here the direct identification of the binding modes of ThT molecules with the prion peptide GNNQQNY by using scanning tunneling microscopy (STM). The assembly structures of GNNQQNY were first observed by STM on a graphite surface, and the introduction of ThT molecules to the surface facilitated the STM observations of the adsorption conformations of ThT with peptide strands. ThT molecules are apt to adsorb on the peptide assembly with β -sheet structure and oriented parallel with the peptide strands adopting four different binding modes. This effort could benefit the understanding of the mechanisms of the interactions between labeling species or inhibitory ligands and amyloid peptides, which is keenly needed for developing diagnostic and therapeutic approaches.

KEYWORDS: GNNQQNY, thioflavin T, binding mode, amyloid, labeling molecule, scanning tunneling microscopy



The amyloid peptide assemblies are rich in β -sheet structures,¹ which are associated with the pathogenic toxicity.² A number of organic species have been tested as molecular probes for studying fibril formation processes^{3,4} and suggested to affect fibrillization in vitro^{5–7} and in vivo,^{8,9} which have inspired great interest in developing potential diagnostic and therapeutic strategies. The labeling molecules have enabled molecular imaging techniques such as fluorescence, positron emission tomography (PET)¹⁰ to gain molecular level insight of binding characteristics to amyloid deposits. Thioflavin T (ThT), as one of the widely used fluorescence labeling species with amyloid complex forming enhanced fluorescence, usually is used to study in situ kinetics of amyloid formation processes.^{11–15} It has been reported that fluorescence efficiency is strongly dependent on the conformation of ThT and the deviation from planar conformation may lead to dramatic reduction of fluorescence of ThT molecules.⁸ The conformation of the ThT molecules could be affected by the methyl group attached to the nitrogen atom of the benzothiazole moiety¹⁶ and rotation of the benzamine moiety around the C–C bond⁴ when binding with amyloid. However, the molecular mechanism is still not clear until now. In addition, recent studies suggest that ThT could be applied promisingly to destabilize the amyloid fibrils for potential therapeutical applications.¹⁷ Therefore, it is an important issue to identify the possible binding sites, molecular orientations, and conformations of the labeling molecules upon binding with amyloid peptides.

The interaction between probe molecules and amyloid peptides has been widely studied by a number of techniques,

including X-ray diffraction (XRD),^{18–20} fluorescence,²¹ circular dichroism,²² isothermal titration calorimetry,^{18,22,23} confocal microscopy,¹¹ molecular dynamics simulation,^{24,25} and computational modeling.^{21,26} Several binding configurations have been proposed on the basis of theoretical and experimental studies. The central pore region of amyloid fibrils is one of the proposed binding locations determined by small-angle X-ray scattering and XRD.^{18,19} The “channel” binding site formed by side chains of residues along the fibril axis have also been shown by many reports, which suggested the perpendicular orientation of the labeling molecular axes to the peptide strands.^{11,21,22,24,25} The parallel orientation of probe molecules to the peptide strands is another proposed binding mode, which is paid more attention in the recently published theoretical studies.^{20,24–26} The proposed three binding modes are yet to be clarified at the molecular level because of the lack of direct evidence from structural analysis that is considerably challenging in both crystal and solution states.

Recently, the progress of using scanning tunneling microscopy (STM) to observe peptide assemblies at liquid–solid interfaces^{27–30} provides a possible venue to obtain amyloid peptide structures with submolecular resolution. The core regions of β -sheet structures have been clearly resolved with STM for the assemblies of amyloid peptides.^{27,29} Such progress could also enable the exploration of the interactions between the labeling molecules and peptides. The possibility of visualizing the core

Received: January 27, 2011

Accepted: March 30, 2011

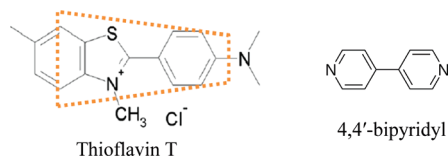
Published: March 30, 2011

regions of peptide sequence would enable molecular level insight of the interaction between probe molecules and peptides, thus providing complementary knowledge on bind processes in fibrillar states.

Extensive studies have shown the misfolded structures of the yeast protein Sup35 to form the $[\text{PSI}^+]$ prion.^{1,31} The Q/N rich fibril forming fragment (GNNQQNY) is from the N terminus of the prion-determining domain of Sup35, which is responsible for prion formation. The fibrils formed by GNNQQNY display the common features of amyloid fibrils:³¹ unbranched morphology, the cross- β diffraction pattern, and binding of the dye molecules Congo red (CR) and ThT. The XRD studies of GNNQQNY reveal characteristic parallel β -sheet structures with the side groups of the residues distributed at both sides of the β -sheet and interdigitated to form steric zippers that stabilize the inter-sheet complexes.³¹ The structural and chemical characteristics of the residues are therefore crucial in the formation of such steric zippers among β -sheets.^{1,32} Such crystalline peptide structures involve interactions between similar residues. It could be expected that further exploration of the interactions between amyloid peptides and labeling organic species could enrich the understanding of the assembly mechanism and the aggregation process of amyloid peptides.

The current study is motivated by the need to unveil the binding modes of labeling molecules at molecular level with amyloid fibrils. ThT is chosen as a model labeling species in this study, whose overall molecular shape would be like a trapezoid as illustrated in Scheme 1. With the observations of amyloid peptide

Scheme 1. Molecular Structures of Thioflavin T (ThT) and 4,4'-Bipyridyl (4Bpy)^a



^a In ThT chemical structures, the benzothiazole group is larger than the dimethylaniline group considering the local density of electronic states, as shown in the dashed trapezoid marked.

assemblies²⁹ and organic molecules,³³ it is now feasible to investigate the assembling of peptides, such as GNNQQNY, and to unveil the detailed binding features between labeling molecules and the peptides. In order to identify the relative location of ThT molecules on peptide assembly, 4,4'-bipyridyl (4Bpy) molecules (Scheme 1) are introduced into the system to label the C termini of the prion peptides due to the strong hydrogen bond formation between N atoms on 4Bpy and C termini of peptides.³⁴ The STM observations suggest that binding of ThT molecules to GNNQQNY peptides could be described by modes with notable differences in adsorption configurations and populations.

RESULTS AND DISCUSSION

The prion fragment GNNQQNY assembly has been observed with lamella characteristics in STM images (Figure S1A in the Supporting Information). This is in analogy to the previous STM observations of the amyloid peptides (β -amyloid²⁷ and amylin²⁹). The peptides are arranged with their molecular axes approximately perpendicular to the long axis of the lamella. It has been known that only stably adsorbed molecular species could be achieved with high-resolution STM images under ambient conditions, and the structural fluctuations of the residue groups in the peptide assemblies could obscure the structural details reflected as contrast in STM images, resulting in less quantitative fine features that could be attributed to the specific residue groups.

In order to identify the C-terminus of the peptide, the coassembly molecule 4Bpy (Scheme 1) has been introduced in our studies.³⁴ Figure 1A is a typical STM image of the coassemblies of GNNQQNY and 4Bpy on a highly orientated pyrolytic graphite (HOPG) surface. Since the conjugated π -electron moieties of 4Bpy lead to enhanced contrast in STM images, 4Bpy molecules can be associated with the linear arrays with relatively high contrast. The stripes with reduced contrast in the middle of two neighboring strings of 4Bpy are consisted of GNNQQNY peptides arranged in head-to-head configurations, similar to the previously reported STM observations of organic molecular assemblies.³⁵ The high-resolution STM image in Figure 1B illustrates the formation of the heterogeneous

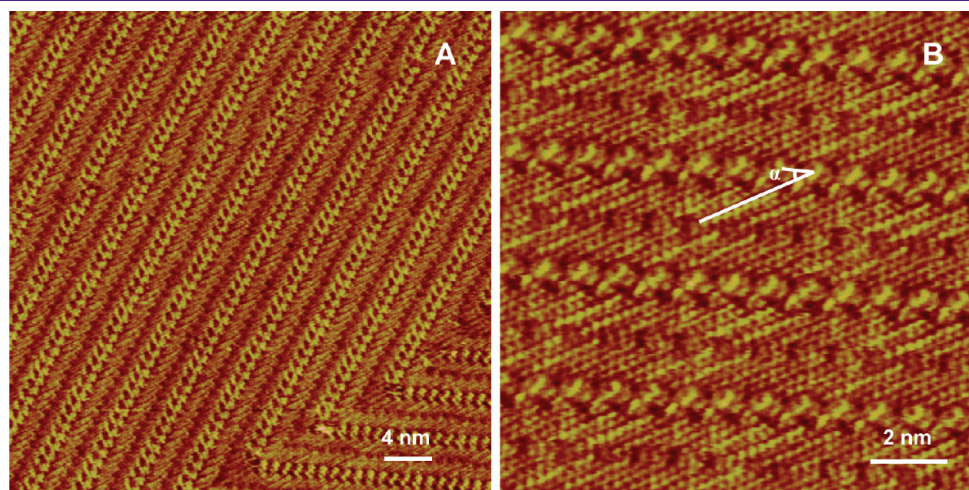


Figure 1. Large-scale (A) and high-resolution (B) STM images of GNNQQNY/4Bpy coassembly. Tunneling conditions: $I = 329.6$ pA, $V = 880.0$ mV. The angle α in (B) represents the angle between peptide strand axes and the lamella direction.

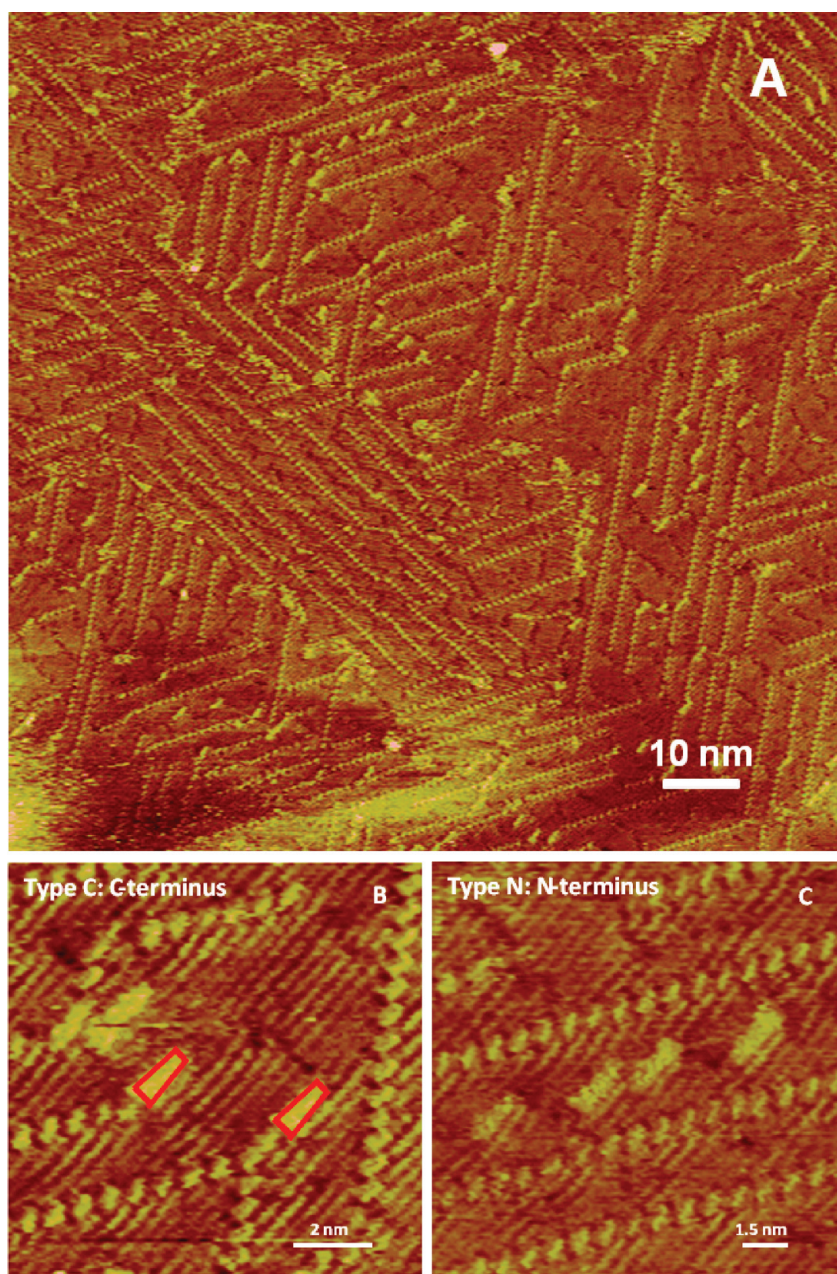


Figure 2. (A) Large-scale STM image of ThT binding to GNNQQNY/4Bpy coassembly. (B, C) High-resolution STM images of type C and type N binding modes of ThT bound to GNNQQNY peptides tagged with 4Bpy. Tunneling conditions: $I = 341.7$ pA, $V = 832.4$ mV. The adsorbed ThT molecules are highlighted by the red trapezoids.

organic-peptide assembly structure which is facilitated by the strong $N \cdots H-O$ hydrogen bond between 4Bpy and the C-terminus of GNNQQNY. This kind of hydrogen bond has been proved to be very stable up to 165 °C characterized by variable-temperature Fourier transform infrared spectroscopy (FTIR).³⁶ The angle α between peptide strand axes and the lamella direction is measured to be $28 \pm 2^\circ$, as the reflection of the hydrogen bond interaction between terminal functional groups.^{37,38} The lengths of GNNQQNY peptides are measured to be 2.4 ± 0.1 nm which is consistent with the expected extended peptide strand length. (Figure S2 in the Supporting Information). The distance between neighboring strands are measured to be 0.47 ± 0.02 nm, which is consistent with the

reported values for β -sheet structures by XRD and STM techniques.^{1,29} The observation of parallel β -sheet structure of GNNQQNY peptides may make it feasible for studying site-specific interaction of labeling molecules by using STM.

It has been known that benzothiazole dye ThT displays a strong increase in fluorescence upon binding to amyloid fibrils and has hence become the most commonly used amyloid-specific labeling agent.^{11,13,15,17,39} Therefore, the direct identification of the binding behaviors of ThT with peptide strands at the molecular level would be very interesting. The large-scale STM image (Figure 2A and Figure S5A in the Supporting Information) illustrates the binding modes of the labeling molecules ThT with GNNQQNY peptides. The ThT molecules

(bright spots) are randomly distributed in STM images. The ThT molecular axes are oriented predominantly parallel to the GNNQQNY strands, which could be clearly differentiated from the linear arrays of 4Bpy molecules. The angle between the ThT molecular axes and the peptide strands is measured to be $0 \pm 3^\circ$. Since the C-termini of the GNNQQNY strands were tagged with 4Bpy molecules, the binding sites of ThT molecules can be clearly observed in the typical high-resolution STM images (Figure 2B and C). Moreover, the ThT molecules appear as a trapezoid (~ 1.5 nm in length) with different-sized molecular ends (Scheme 1). In addition to the major parallel binding modes, a small fraction ($< 5\%$) of ThT molecules are observed to be immobilized into the trough between two stripes of GNNQQNY peptides or regions of N-termini, or at domain boundaries which commonly occurs in coadsorption structures.

The adsorption configurations of labeling molecules to peptide strands have been proposed in a number of previous simulation studies.^{24,26} In the earlier molecular model, it is suggested that the labeling molecule CR intercalates between two peptide monomers at an interface formed by a pair of antiparallel peptide strands.²⁶ In some molecular dynamics simulations, the binding sites observed were either at the ends of the fibril or on top of the β -strand.^{24,25} In the current study with STM molecular level observations on the binding modes of ThT with GNNQQNY peptides, the parallel binding configurations could be further characterized as two binding modes: type C is next to the C-termini of the GNNQQNY strands and type N is next to the N-termini (Figure 2B and C).

It has been suggested that there may exist a “channel” binding mode that ThT binds to peptide assemblies along the axis of amyloid fibril in the previous studies by confocal microscopy,¹¹ XRD study,²¹ and modeling analysis.²⁵ The binding characteristics of ThT molecules to the channels formed by amino acid residue groups in amyloid fibrils could be affected by the shape complementarities between the channels. Such “channel” binding modes could not be found in our STM observations possibly due to the fact that the proposed “channel” structures in aggregated fibrils form may not be available for the monolayer assembly of surface-bound peptides in the present study. In addition, the presence of 4Bpy could also change the relative registration of the peptides within lamellae, which could be reflected in the tilt angle between GNNQQNY molecular axes and the lamella direction for the coassembled structures ($28 \pm 2^\circ$ in Figure 1B) compared to nearly 90° in the pristine peptide assemblies. Despite structural differences of peptide assemblies in solution and at the solution–solid interface, the observed binding effects of ThT on surface-bound peptide assemblies could still be useful to elucidate the localized interactions between labeling species and various residues of peptides. The underlining mechanisms for binding behaviors at the molecular level are definitely worthy of further studies.

Based on the high-resolution STM images (Figure 2B and C) and the chemical structures of ThT (Scheme 1), the wider end of ThT molecules could be ascribed to the benzothiazole group as highlighted by the red trapezoids. In binding type C, the wider end (benzothiazole group) is preferentially situated close to the C-termini of GNNQQNY strands. This binding mode may be associated with the dipole–dipole interaction between the benzothiazole groups of ThT molecules and C-termini of GNNQQNY peptides. The statistical result shows the higher number frequency of orientations with the benzothiazole groups next to the C-termini of peptides than those of dimethylaniline

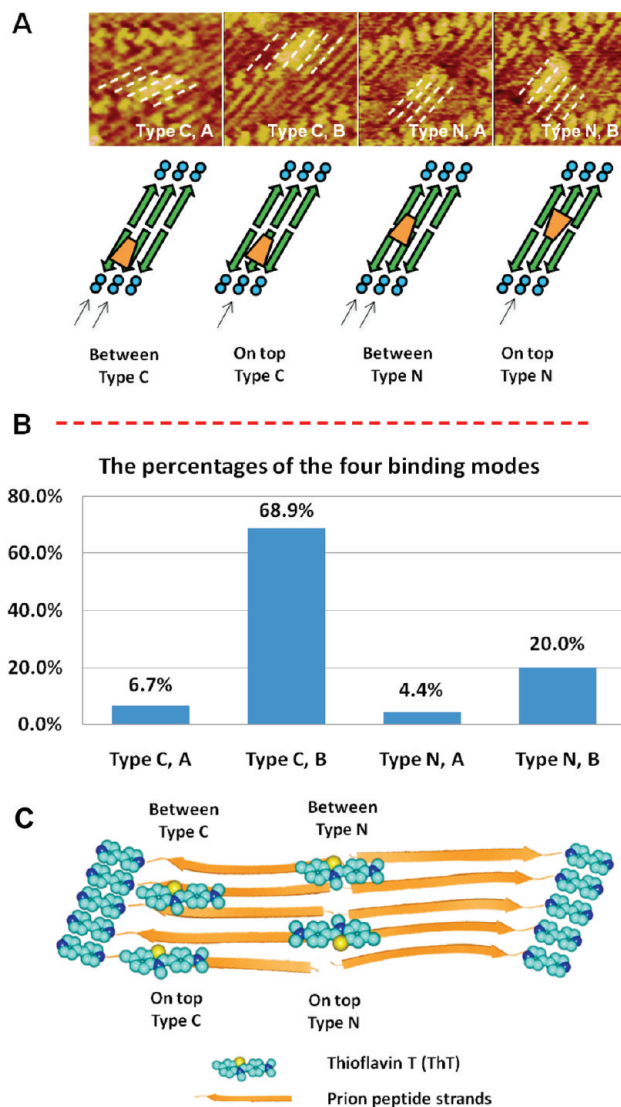


Figure 3. (A) High-resolution STM images ($6 \text{ nm} \times 6 \text{ nm}$) and the corresponding schematic diagrams for the different binding modes of ThT molecules. The dashed lines in the upper STM images point out the peptide orientations. In the lower schematic diagrams, the “8” shaped features with two blue circles stand for the 4Bpy molecules, the orange trapezoids for the ThT molecules, and the green arrows for the peptide strands. The thin black arrows in the lower schematics point out the peptide strands involved in the ThT binding. (B) Statistical results of the percentages for the corresponding binding modes in (A). (C) Schematic illustration of the binding modes of ThT with GNNQQNY/4Bpy coassembly. The backbones of the peptide strands are represented by orange arrows. Yellow, cyan, and blue color represent S, C, and N atoms, respectively.

groups (Figure S3 in the Supporting Information), which may explain the specific binding modes for the ThT molecule. In binding type N, the ThT molecules are adsorbed across two neighboring rows of peptide assembly (Figure 2C) and thus the orientation of the ThT molecules is equivalent with even distribution.

Close examination of the distribution of the adsorbed ThT molecules further reveals four possible binding sites as shown in Figure 3A and Figure S5B in the Supporting Information. Type C is close to the C-termini as marked by the 4Bpy, and type N is

close to the N-terminal represented by the trench regions in the assemblies. The binding affinities of the two binding sites are different according to the ratio of adsorbates (type C/type N = 68:22 (number frequency) = 76%:24%; Figure 3B) in STM images. Furthermore, the relative binding configurations of the ThT molecules to peptide molecules could be identified from STM images. As illustrated in Figure 3A, the ThT molecules are bound either intercalating between two adjacent peptide chains (mode A) or directly on top of the peptide chains (mode B), and both have been proposed previously.^{24–26} Four binding modes are illustrated in the schematic diagram in Figure 3A. It is also noticeable in our STM observations that the majority of ThT molecules are bound directly on top of the peptide strands (mode B) rather than in the locations between the peptide chains (mode A) according to the ratio of adsorbate (A/B = 10:80 (number frequency) = 11%:89%/ Figure 3B and Figure S4 in the Supporting Information). The detailed results for the ThT binding modes have been concluded in the histogram in Figure 3B and Figure S4 in the Supporting Information. In the four binding modes for the ThT molecules with parallel configuration, binding next to the C-terminus and on top of peptide strands is the preferential binding mode accounting for 69% in the statistical results. The preferential binding of the benzothiazole moiety of ThT molecules to the C-termini of peptides could be explained as the electrostatic attraction between positively charged moieties and negatively charged carboxyl groups by partial deprotonation under ambient conditions. The specific binding could also be associated with the hydrogen bond formation between ThT molecules and the C-termini residues Y and/or N. The schematic diagram of the ThT molecules binding to the GNNQQNY/4Bpy coassembly has been illustrated in Figure 3C.

In this STM work, several specific binding modes of ThT with GNNQQNY strands have been identified at the molecular level. It may be noticed that the assembly configurations for surface-bound peptide assemblies could differ from the fibrillar structures considering the two-dimensional nature of the surfaces. Because the binding environments for probe molecules may be varied, some of the binding modes proposed in previous studies could be possibly discernible in STM investigations. Several points could be inferred from the current study: the ThT molecules are mixed previously in the peptide solution before the STM observation, which is similar to the ThT assay; the binding results are obtained at liquid–solid interfaces, where the water molecules may still be involved in by surrounding peptide assemblies; the high-resolution STM images could give the molecular-level evidence on the binding modes of labeling molecules and amyloid aggregation inhibitors as well, which is challenging by using crystallography and spectroscopic studies for amyloids. Therefore, this binding mode work may be helpful for realizing the molecular mechanisms of ThT fluorescence enhanced assay as well as amyloid aggregation and inhibition pathways interfered by inhibitors.

CONCLUSIONS

In summary, the assembly structures of GNNQQNY have been observed using STM. ThT molecules are found to adsorb on the GNNQQNY β -sheet structure and parallel to the peptide strands. Four different binding modes of ThT to the peptide chains of GNNQQNY are identified. This effort could help obtain complementary insight of the peptide sequence effect or other structural and chemical effects on the interaction

characteristics of labeling species, and binding mechanisms of inhibitory ligands associated with amyloid aggregation and toxicity, which are keenly needed for developing diagnostic and therapeutic approaches.

METHODS

Sample Preparation. Synthetic peptide (GNNQQNY) was dissolved in chromatographic grade acetonitrile (ACN) to a concentration of 1 mg/mL (Supporting Information). A total of 1 μ L of solution was deposited on a freshly cleaved HOPG surface. STM experiments were performed after the solvent ACN was evaporated from the HOPG surface.

GNNQQNY (1 mg) and the solid powder of 4Bpy (1 mg) were dissolved in ACN (1 mL) to a concentration of 1 mg/mL. An amount of 1 μ L of solution was deposited on HOPG immediately after mixing. In the binding experiments, the labeling molecule ThT (0.1 mg/mL) was first mixed with the solution of GNNQQNY and 4Bpy. Then 1 μ L of mixed solution was deposited on HOPG surface and followed by the similar procedure.

STM Measurements. STM experiments were performed in constant-current mode under ambient conditions (Nanoscope IIIa scanning probe microscope (SPM) system, Veeco). The tips were mechanically formed Pt/Ir wire (80%/20%). The STM tunneling conditions are described in the corresponding figure captions. Experiments were repeated more than five times independently using different tips.

Statistical Methods. The lengths of the peptide strands in STM images are measured by using the Nanoscope software. A step size of 0.325 nm for every residue is assumed in the statistical histogram of the length distribution of the peptide assemblies, which is fitted by Gaussian distribution. The measured lengths in the histograms represent the average value of the independent experiments. The number frequencies in the statistical results are all based on number of events. The statistical results for the binding modes are derived from many STM images.

ASSOCIATED CONTENT

Supporting Information. STM images of GNNQQNY; histogram of statistical distribution for length measurements of GNNQQNY peptides; plot showing frequency of binding orientation of ThT molecules in Type C; table of statistical results of the number of frequencies for binding modes in Figure 3A; STM images of ThT binding to GNNQQNY/4Bpy co-assembly. This material is available free of charge via the Internet at <http://pubs.acs.org>.

AUTHOR INFORMATION

Corresponding Author

*(Y.Y.) Telephone: +86-10-82545559. Fax: +86-10-62656765. E-mail: yangyl@nanocr.cn. (C.W.) Telephone: +86-10-82545561. Fax: +86-10-62656765. E-mail: wangch@nanocr.cn.

Funding Sources

This work was supported by the National Basic Research Program of China (2009CB930100, 2011CB932800) and Chinese Academy of Sciences (KJCX2-YW-M15). Financial support from National Natural Science Foundation of China (209111-30229) is also gratefully acknowledged.

REFERENCES

(1) Sawaya, M. R., Sambashivan, S., Nelson, R., Ivanova, M. I., Sievers, S. A., Apostol, M. I., Thompson, M. J., Balbirnie, M., Wiltzius,

- J. J., McFarlane, H. T., Madsen, A. O., Riek, C., and Eisenberg, D. (2007) Atomic structures of amyloid cross-beta spines reveal varied steric zippers. *Nature* 447 (7143), 453–457.
- (2) Bucciantini, M., Giannoni, E., Chiti, F., Baroni, F., Formigli, L., Zurdo, J. S., Taddei, N., Ramponi, G., Dobson, C. M., and Stefani, M. (2002) Inherent toxicity of aggregates implies a common mechanism for protein misfolding diseases. *Nature* 416 (6880), 507–511.
- (3) Stains, C. I., Mondal, K., and Ghosh, I. (2007) Molecules that target beta-amyloid. *ChemMedChem* 2 (12), 1674–1692.
- (4) Groenning, M. (2009) Binding mode of Thioflavin T and other molecular probes in the context of amyloid fibrils-current status. *J. Chem. Biol.* 3, 1–18.
- (5) Heiser, V., Scherzinger, E., Boeddrich, A., Nordhoff, E., Lurz, R., Schugardt, N., Lehrach, H., and Wanker, E. E. (2000) Inhibition of huntingtin fibrillogenesis by specific antibodies and small molecules: Implications for Huntington's disease therapy. *Proc. Natl. Acad. Sci. U.S.A.* 97 (12), 6739–6744.
- (6) Blanchard, B. J., Chen, A., Rozeboom, L. M., Stafford, K. A., Weigele, P., and Ingram, V. M. (2004) Efficient reversal of Alzheimer's disease fibril formation and elimination of neurotoxicity by a small molecule. *Proc. Natl. Acad. Sci. U.S.A.* 101 (40), 14326–14332.
- (7) Yang, F. S., Lim, G. P., Begum, A. N., Ubeda, O. J., Simmons, M. R., Ambegaokar, S. S., Chen, P. P., Kaye, R., Glabe, C. G., Frautschi, S. A., and Cole, G. M. (2005) Curcumin inhibits formation of amyloid beta oligomers and fibrils, binds plaques, and reduces amyloid in vivo. *J. Biol. Chem.* 280 (7), 5892–5901.
- (8) Ritchie, C. W., Bush, A. I., Mackinnon, A., Macfarlane, S., Mastwyk, M., Macgregor, L., Kiernan, L., Cherny, R., Li, Q. X., Tammer, A., Carrington, D., Mavros, C., Volitakis, I., Xilinas, M., Ames, D., Davis, S., Volitakis, I., Xilinas, M., Ames, D., Davis, S., Beyreuther, K., Tanzi, R. E., and Masters, C. L. (2003) Metal-protein attenuation with iodochlorhydroxyquin (clioquinol) targeting A beta amyloid deposition and toxicity in Alzheimer disease - A pilot phase 2 clinical trial. *Arch. Neurol.* 60 (12), 1685–1691.
- (9) Porat, Y., Abramowitz, A., and Gazit, E. (2006) Inhibition of amyloid fibril formation by polyphenols: structural similarity and aromatic interactions as a common inhibition mechanism. *Chem. Biol. Drug Des.* 67 (1), 27–37.
- (10) Lockhart, A., Ye, L., Judd, D. B., Merritt, A. T., Lowe, P. N., Morgenstern, J. L., Hong, G., Gee, A. D., and Brown, J. (2005) Evidence for the presence of three distinct binding sites for the thioflavin T class of Alzheimer's disease PET imaging agents on beta-amyloid peptide fibrils. *J. Biol. Chem.* 280 (9), 7677–7684.
- (11) Krebs, M. R. H., Bromley, E. H. C., and Donald, A. M. (2005) The binding of thioflavin-T to amyloid fibrils: localisation and implications. *J. Struct. Biol.* 149 (1), 30–37.
- (12) Dzwolak, W., and Pecul, M. (2005) Chiral bias of amyloid fibrils revealed by the twisted conformation of Thioflavin T: An induced circular dichroism/DFT study. *FEBS Lett.* 579 (29), 6601–6603.
- (13) Ban, T., Hamada, D., Hasegawa, K., Naiki, H., and Goto, Y. (2003) Direct observation of amyloid fibril growth monitored by thioflavin T fluorescence. *J. Biol. Chem.* 278 (19), 16462–16465.
- (14) Urbanc, B., Cruz, L., Le, R., Sanders, J., Ashe, K. H., Duff, K., Stanley, H. E., Irizarry, M. C., and Hyman, B. T. (2002) Neurotoxic effects of thioflavin S-positive amyloid deposits in transgenic mice and Alzheimer's disease. *Proc. Natl. Acad. Sci. U.S.A.* 99 (22), 13990–13995.
- (15) Klunk, W. E., Wang, Y. M., Huang, G. F., Debnath, M. L., Holt, D. P., and Mathis, C. A. (2001) Uncharged thioflavin-T derivatives bind to amyloid-beta protein with high affinity and readily enter the brain. *Life Sci.* 69 (13), 1471–1484.
- (16) Turoverov, K. K., Kuznetsova, I. M., Maskevich, A. A., Stepuro, V. I., Kuzmitsky, V. A., and Uversky, V. N. (2007) ThT as an instrument for testing and investigation of amyloid and amyloid-like fibrils. *Int. Conf. Lasers, Appl. Technol.* 6733, R7331.
- (17) Ozawa, D., Yagi, H., Ban, T., Kameda, A., Kawakami, T., Naiki, H., and Goto, Y. (2009) Destruction of Amyloid Fibrils of a beta(2)-Microglobulin Fragment by Laser Beam Irradiation. *J. Biol. Chem.* 284 (2), 1009–1017.
- (18) Groenning, M., Norrman, M., Flink, J. M., van de Weert, M., Bukrinsky, J. T., Schluckebier, G., and Frokjaer, S. (2007) Binding mode of Thioflavin T in insulin amyloid fibrils. *J. Struct. Biol.* 159 (3), 483–497.
- (19) Harel, M., Sonoda, L. K., Silman, I., Sussman, J. L., and Rosenberry, T. L. (2008) Crystal structure of thioflavin T bound to the peripheral site of Torpedo californica acetylcholinesterase reveals how thioflavin T acts as a sensitive fluorescent reporter of ligand binding to the acylation site. *J. Am. Chem. Soc.* 130 (25), 7856–7861.
- (20) Turnell, W. G., and Finch, J. T. (1992) Binding of the Dye Congo Red to the Amyloid Protein Pig Insulin Reveals a Novel Homology Amongst Amyloid-Forming Peptide Sequences. *J. Mol. Biol.* 227 (4), 1205–1223.
- (21) Biancalana, M., Makabe, K., Koide, A., and Koide, S. (2009) Molecular Mechanism of Thioflavin-T Binding to the Surface of beta-Rich Peptide Self-Assemblies. *J. Mol. Biol.* 385 (4), 1052–1063.
- (22) Sabate, R., Lascu, I., and Saupe, S. J. (2008) On the binding of Thioflavin-T to HET-s amyloid fibrils assembled at pH 2. *J. Struct. Biol.* 162 (3), 387–396.
- (23) Groenning, M., Olsen, L., van de Weert, M., Flink, J. M., Frokjaer, S., and Jorgensen, F. S. (2007) Study on the binding of Thioflavin T to beta-sheet-rich and non-beta-sheet cavities. *J. Struct. Biol.* 158 (3), 358–369.
- (24) Wu, C., Wang, Z. X., Lei, H. X., Zhang, W., and Duan, Y. (2007) Dual binding modes of Congo red to amyloid protofibril surface observed in molecular dynamics simulations. *J. Am. Chem. Soc.* 129 (5), 1225–1232.
- (25) Wu, C., Wang, Z. X., Lei, H. X., Duan, Y., Bowers, M. T., and Shea, J. E. (2008) The Binding of Thioflavin T and Its Neutral Analog BTA-1 to Protofibrils of the Alzheimer's Disease A beta(16-22) Peptide Probed by Molecular Dynamics Simulations. *J. Mol. Biol.* 384 (3), 718–729.
- (26) Carter, D. B., and Chou, K. C. (1998) A model for structure-dependent binding of Congo red to Alzheimer beta-amyloid fibrils. *Neurobiol. Aging* 19 (1), 37–40.
- (27) Ma, X. J., Liu, L., Mao, X. B., Niu, L., Deng, K., Wu, W. H., Li, Y. M., Yang, Y. L., and Wang, C. (2009) Amyloid-beta (1-42) Folding Multiplicity and Single Molecule Binding Behavior Studied by STM. *J. Mol. Biol.* 388, 894–901.
- (28) Matmour, R., De Cat, I., George, S. J., Adriaens, W., Leclere, P., Bomans, P. H. H., Sommerdijk, N., Gielen, J. C., Christianen, P. C. M., Heldens, J. T., van Hest, J. C. M., Lowik, D., De Feyter, S., Meijer, E. W., and Schenning, A. P. H. J. (2008) Oligo(p-phenylenevinylene)-Peptide Conjugates: Synthesis and Self-Assembly in Solution and at the Solid-Liquid Interface. *J. Am. Chem. Soc.* 130 (44), 14576–14583.
- (29) Mao, X. B., Ma, X. J., Liu, L., Niu, L., Yang, Y. L., and Wang, C. (2009) Structural characteristics of the beta-sheet-like human and rat islet amyloid polypeptides as determined by scanning tunneling microscopy. *J. Struct. Biol.* 167 (3), 209–215.
- (30) Mao, X. B., Wang, Y. B., Liu, L., Niu, L., Yang, Y. L., and Wang, C. (2009) Molecular-Level Evidence of the Surface-Induced Transformation of Peptide Structures Revealed by Scanning Tunneling Microscopy. *Langmuir* 25 (16), 8849–8853.
- (31) Nelson, R., Sawaya, M. R., Balbirnie, M., Madsen, A. O., Riek, C., Grothe, R., and Eisenberg, D. (2005) Structure of the cross-beta spine of amyloid-like fibrils. *Nature* 435 (7043), 773–778.
- (32) Ivanova, M. I., Sievers, S. A., Sawaya, M. R., Wall, J. S., and Eisenberg, D. (2009) Molecular basis for insulin fibril assembly. *Proc. Natl. Acad. Sci. U.S.A.* 106 (45), 18990–18995.
- (33) Liu, L., Zhang, L., Mao, X., Niu, L., Yang, Y., and Wang, C. (2009) Chaperon-Mediated Single Molecular Approach Toward Modulating A beta Peptide Aggregation. *Nano Lett.* 9 (12), 4066–4072.
- (34) Mao, X. B.; Wang, C. X.; Ma, X. J.; Zhang, M.; Liu, L.; Zhang, L.; Niu, L.; Zeng, Q. D.; Yang, Y. L.; Wang, C. Molecular level studies on binding modes of labeling molecules with polyalanine peptides. *Nano-scale* 2011, DOI: 10.1039/c0nr00782j.
- (35) Xu, B., Yin, S. X., Wang, C., Zeng, Q. D., Qiu, X. H., and Bai, C. L. (2001) Identification of hydrogen bond characterizations of isomeric 4Bpy and 2Bpy by STM. *Surf. Interface Anal.* 32, 245–247.

(36) Ma, X. J., Shen, Y. T., Deng, K., Tang, H., Lei, S. B., Wang, C., Yang, Y. L., and Feng, X. Z. (2007) Matrix-molecule induced chiral enhancement effect of binary supramolecular liquid crystals. *J. Mater. Chem.* 17 (44), 4699–4704.

(37) Claypool, C. L., Faglioni, F., Goddard, W. A., Gray, H. B., Lewis, N. S., and Marcus, R. A. (1997) Source of image contrast in STM images of functionalized alkanes on graphite: A systematic functional group approach. *J. Phys. Chem. B* 101 (31), 5978–5995.

(38) Cyr, D. M., Venkataraman, B., Flynn, G. W., Black, A., and Whitesides, G. M. (1996) Functional group identification in scanning tunneling microscopy of molecular adsorbates. *J. Phys. Chem.* 100 (32), 13747–13759.

(39) Yona, R. L., Mazeris, S., Faller, P., and Gras, E. (2008) Thioflavin derivatives as markers for amyloid-beta fibrils: Insights into structural features important for high-affinity binding. *ChemMedChem* 3 (1), 63–66.